Temperature dependence of the far-infrared reflectance spectra of Si:P near the metal-insulator transition

A. Gaymann* and H. P. Geserich
Institut für Angewandte Physik, Universität Karlsruhe, D-76128 Karlsruhe, Germany

H. v. Löhneysen
Physikalisches Institut, Universität Karlsruhe, D-76128 Karlsruhe, Germany
(Received 1 May 1995; revised manuscript received 20 July 1995)

We report on far-infrared reflection measurements on Si:P in the temperature range between 10 and 300 K for doping concentrations between $N = 3.4 \times 10^{17}$ cm^{-3} and 7.4×10^{19} cm^{-3}, thus including the metal-insulator transition occurring near $N_c = 3.5 \times 10^{18}$ cm^{-3}. At 300 K all samples show only the well-known free-carrier absorption where the carriers are thermally activated into the conduction band. At 10 K, for samples with very low-doping concentrations, optical transitions to donor $2p$ states and to the conduction band are observed. Metallic samples show at 10 K interband transitions giving evidence for the existence of central-cell effects in the metallic phase, i.e., transitions between the $1s(A_1)$ ground state and the closely spaced $1s(E)$ and $1s(T_2)$ states. The occupation of the $1s$ and the conduction-band states as a function of temperature can be deduced from the oscillator strengths of the corresponding interband transitions. These results strongly suggest that at the metal-insulator transition, the impurity band is still separated energetically from the conduction band.

I. INTRODUCTION

Within the field of metal-insulator transitions (MIT), investigations on doped semiconductors like Si:P have been of particular interest for many years. These systems have become model substances for studying a MIT driven by the combined effect of disorder and electron-electron interactions, which still is far from being completely understood.[1]

The distinction between the metallic and the insulating state is only sharp for $T \to 0$. As a consequence, a lot of work has been devoted to study the MIT in doped semiconductors below 1 K. Thermodynamic properties like the magnetization and the specific heat, and transport properties like dc conductivity, thermoelectric power, and ac conductivity have been investigated, all of them probing the ground state or very low-lying excitations. By increasing the temperature of the sample, higher levels will be populated leading to further information about these levels and bands. However, even such a fundamental question as whether at the MIT the impurity band has merged with the conduction band or otherwise, has not been resolved until very recently.

In optical measurements in the far- and mid-infrared region, the energy scale is extended to higher values, probing not only the electron transport properties, but also the density of states of the different impurity levels. However, up to now, only a few papers have dealt with the temperature dependence of the optical spectra on impurity states or impurity bands. Thirty years ago, Aggarwal studied the excitation spectra from the doublet $1s(E)$ and the triplet $1s(T_2)$ levels of group V donors in silicon.[2] The spectra have been measured at a temperature sufficiently high to populate the higher valley-orbit split $1s$ states. The energetical position of the two states was inferred from the relative intensities of transitions to the same excited state.

The valley-orbit Raman spectrum of phosphorous-doped silicon was studied systematically by Jain *et al.*[3] The observed temperature dependence of the spectra can be qualitatively understood in terms of temperature-dependent occupation probabilities. For N just below N_c, the remnant of the valley-orbit line, i.e., a weak shoulder vanishes quickly with increasing T. This is explained by the thermal depopulation of the $1s(A_1)$ states.[3]

In a previous paper, we have reported on the reflectance spectra of Si:P at 10 K. There, we could demonstrate that the impurity band is formed by the overlap of the $1s(A_1)$ ground states and is well separated from the conduction band when the MIT occurs.[4] Only far beyond the metallic limit the impurity band merges with the conduction band.

In this paper, we present a comprehensive account of our reflection measurements on uncompensated Si:P in the temperature range between 10 K and 300 K. The study covers more than two orders of magnitude in doping density. It will be shown that all the structures observed can be identified unambiguously, with respect to the underlying optical transitions.

II. EXPERIMENT

Phosphorous-doped single crystals were obtained from Wacker Chemitronic, Burghausen, Germany. They were

grown with the Czochralski method, yielding rods of 54 mm in diameter. Taking advantage of a P concentration gradient along the axis of the rods, several samples with different N could be conveniently cut from a single rod, using a diamond saw. N was determined by the room-temperature resistivity ρ_{295}, using the calibration of Thurber *et al.*[6] As usual, a fit of the resistance ratio $R(295\,\mathrm{K})/R(4.2\,\mathrm{K})$ vs ρ_{295} was employed for a more accurate concentration determination. The samples with typical dimensions of $9 \times 9 \times 4$ mm^3 were polished with diamond powder to obtain a clean and planar surface.

Far- and mid-infrared reflection measurements were performed using a Fourier transform spectrometer *Bruker IFS 113v*. The spectral range was varied between 2 meV and 620 meV ($20\,\mathrm{cm}^{-1}$ – $5000\,\mathrm{cm}^{-1}$). A black polyethylene filter eliminated radiation above 1 eV.

The samples were mounted in a helium-flow cryostat, with thin polyethylene windows. Sample cooling was achieved by helium exchange gas ($p \approx 10$ mbar). The temperature was measured with an AuFe-Cr thermocouple mounted on the sample holder.

At each temperature, the radiation reflected from the sample at near-normal incidence was compared to that reflected from a gold mirror. Identical positioning of sample and mirror was attained by laser adjustment and a special turning mechanism. The absolute photometric accuracy of the reflectance data was better than 1%. There was no heating of the sample by the incident radiation, as determined by an additional platinum resistor mounted directly on a sample surface during a test run.

Furthermore, we have examined whether the free-carrier distribution was changed by photoinduced transitions, due to the broad spectrum of the incident radiation. Upon reducing the intensity of the radiation by more than one order of magnitude, changes of the reflectance spectra neither of the insulating nor of the metallic samples could be observed. Therefore, photoinduced effects could be excluded.

III. ANALYSIS OF OPTICAL REFLECTANCE SPECTRA

Two different methods were used to determine the dielectric function or the conductivity function of the investigated samples. Reflectance spectra at 300 K were fitted using a simplified Drude model (see below). The spectra at intermediate temperatures and at 10 K were evaluated by applying a Kramers-Kronig transformation after having extrapolated the spectra differentiably to higher and lower energies, using a simplified Lorentz-Drude model. The obtained real part of $\sigma(\hbar\omega)$ reflects the joint density of states from which optical transitions can be identified. In order to get quantitative results about the interband transitions and the occupation of the corresponding levels, the whole spectra were fitted using the same Lorentz-Drude model. In addition, this allows a detailed study of the temperature dependence.

As the spectral range of the optical transitions discussed in this work is well below the fundamental absorption edge, the contribution of the fundamental absorption to the dielectric function can be taken into account by a constant value ϵ_∞. The energy-dependent contributions result from free-carrier absorption and from optical transitions between impurity states or between impurity- and conduction-band states.

The free-carrier absorption is described by a Drude term, whereas the transitions involving impurity states can be modeled by Lorentzian oscillators. Therefore, a complete description of the optical properties of Si:P in the spectral range under investigation is given by the following expression:[5]

$$\epsilon(\omega) = \epsilon_\infty \left(1 - \frac{\omega_p^2}{\omega^2 - \mathrm{i}\omega\Gamma}\right) + \sum_j \frac{\omega_{pj}^2}{\omega_{0j}^2 - \omega^2 - \mathrm{i}\Gamma_j\omega}\,, \quad (1)$$

with $\omega_p^2 = ne^2/\epsilon_0\epsilon_\infty m^*_{\mathrm{opt}}$, where n, m^*_{opt}, and Γ denote the carrier concentration, the effective mass, and the scattering rate, i.e., the microscopic parameters of the free carriers. In contrast, the quantities characterizing the Lorentzian oscillators are only used as fitting parameters. A physical interpretation requires quantum-mechanical calculations, where the density of states, the occupation of ground states and final states, matrix elements, and selection rules are taken into consideration.[5] It should be mentioned that due to the random distribution of the doping atoms, the conservation of the wave vector no longer holds for transitions involving impurity-band states.

IV. RESULTS AND DISCUSSION

A. Reflectance spectra at room temperature

The experimental reflectance spectra of all measured samples at room temperature are presented in Fig. 1 (solid lines). All spectra exhibit well-defined plasma edges. Towards low energies, some weak oscillations, due to interference effects arising at the bolometer cutoff filter, are visible.

As expected, the plasma edges shift to higher energy with increasing doping concentration. The dashed lines show that all room-temperature spectra can be described well by a Drude model. This demonstrates that in the investigated spectral range, only intraband transitions are present at 300 K because the excess electrons of the phosphorous impurities are thermally excited into the conduction band. This is true also for the metallic samples, except the highly metallic one ($N = 73.7 \times 10^{18}\,\mathrm{cm}^{-3}$), where a distinction between the impurity band and the conduction band is not possible anymore, since the two bands have merged (see below).

At room temperature, more than 95% of the impurity atoms are ionized for samples in the insulating regime.[7] Thus, the free-carrier concentration n is almost equal to the doping concentration N. This is also true for the metallic samples, where an impurity band has been formed. On this premises, the optical effective masses $m^*_{\mathrm{opt}}(N)$ can be determined from the Drude fits (see Table I).

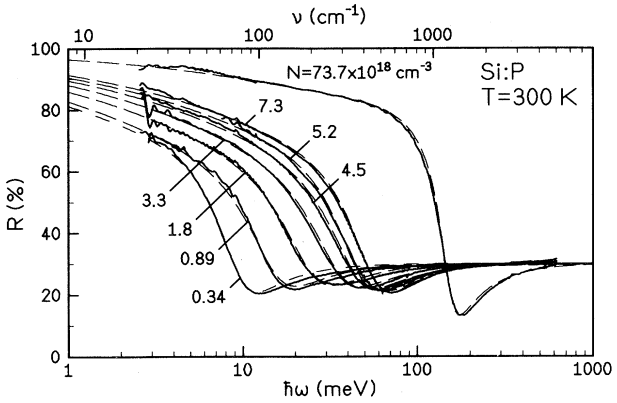

FIG. 1. Reflectance spectra $R(\hbar\omega)$ at 300 K (solid lines) and Drude fits (dashed lines) covering the whole investigated range of doping density.

At doping concentration slightly above N_c, $m^*_{\rm opt} = 0.27m_0$ is obtained as expected from theoretical considerations.[8] For the sample with $N = 73.7 \times 10^{18}\,{\rm cm}^{-3}$, we find an effective mass of $0.36m_0$. This is due to the deviation from the parabolicity of the conduction band at higher energies. This result is in qualitative agreement with earlier measurements.[9–11]

For the samples with $N < N_c$, the deduced effective masses apparently increase with decreasing doping concentration reaching a maximum value of $0.43m_0$ for $N = 0.34 \times 10^{18}\,{\rm cm}^{-3}$. Absorption measurements of Si:P samples in the same regime have yielded the same functional curve for $m^*_{\rm opt}(N)$.[12]

This is in contradiction to the well-known band structure of Si leading to a value of $0.27m_0$ for low-doping concentrations. This deviation may be due to an overestimation of the free-carrier concentration. This could happen as the random distribution of the donor atoms results in the formation of localized tail states at the edges of the conduction band,[13] where a part of the charge carriers are trapped.

In principle, the free-carrier concentration can be obtained by Hall-effect measurements. In the case of doped semiconductors, the simple dependence between n and the Hall constant R_H must be extended by taking a scattering factor $A(N)$ into account, i.e., $R_H = A(N)/en$ (see, e.g., Ref. 14). However, the deviation of $A(N)$ from unity is not sufficient to explain the above discrepancy. A more likely reason is depletion regions in lightly doped samples, which extend more deeply into the bulk material than in heavily doped ones. Together with inhomogeneities, which are stronger in lightly doped samples, too, they may be responsible for the apparent increase of $m^*_{\rm opt}(N)$ with decreasing N. A similar effect was already reported by Palik and Wright,[15] who presented data of the effective mass of InP at very low-doping concentrations determined by cyclotron resonance and Faraday rotation.

From the Drude fit, the mean free time τ and, hence, the mobility $\mu_{\rm opt}(N)$ have been determined, taking into account the deduced effective masses or, more correctly, the $N/m^*_{\rm opt}$ ratio. Table I shows the results. If an effective mass of $0.27m_0$ would be taken for the insulating samples, the deviation would amount to 37% at most and would not change the qualitative $\mu_{\rm opt}(N)$ dependence. The mobility of the electrons decreases with increasing doping concentration, due to the scattering off ionized impurities, while the interaction with phonons is almost independent of N. (The apparent nonmonotonic behavior for $N = 5.2 \times 10^{18}\ {\rm cm}^{-3}$ is within the estimated error bar of ±10%.) The results can be compared with data obtained by resistivity[16] and by resistivity and junction capacitance-voltage measurements.[7] The good agreement between these and our data on the one hand and between the reflectance spectra and the Drude fits on the other hand confirms that the Drude model with the frequency-independent scattering rate is an adequate model in determining the mobility in the present doping regime. Measurements of the Hall mobility $\mu_H = \sigma_{\rm dc}R_H$ show reasonable agreement with the optical data for $\mu_{\rm opt}$ for metallic samples and somewhat larger differences for insulating samples (see Tables I and II). Finally, the conductivity functions extrapolated to the limit $\hbar\omega \to 0$, $\sigma_{\hbar\omega\to 0}$, and measured dc conductivity $\sigma_{\rm dc}$ Ref. 17 yield overall good agreement.

TABLE I. Effective mass $m^*_{\rm opt}$, mean free time τ, mobility $\mu_{\rm opt}$, and extrapolated value of $\sigma_{\hbar\omega\to 0}$ at 300 K, for different Si:P samples, with P concentration N obtained by reflection measurements.

N (10^{18} cm^{-3})	$m^*_{\rm opt}/m_0$	τ (10^{-14} s)	$\mu_{\rm opt}$ (cm^2/V s)	$\sigma_{\hbar\omega\to 0}$ (S/cm)
73.3	0.36	1.4	67.6	800
7.3	0.27	1.7	110	135
5.2	0.27	2.0	126	105
4.5	0.27	1.8	117	94
3.3	(0.29)	2.0	121	66
1.8	(0.34)	3.1	160	46
0.89	(0.42)	5.1	213	30
0.34	(0.43)	10.6	422	23

B. Reflection spectra at low temperatures (10 K)

Figure 2 shows the reflectance spectra of the insulating samples at 10 K. The plasma edges have disappeared or have been shifted to lower energies outside of the spectrometer range, indicating that the carriers are com-

TABLE II. Hall constant R_H, dc conductivity $\sigma_{\rm dc}$, and Hall mobility $\mu_H = \sigma_{\rm dc}R_H$ at 300 K, for the same Si:P samples [measured values of $\sigma_{\rm dc}$ after (Ref. 17)].

N (10^{18} cm^{-3})	R_H (cm^3/C)	$\sigma_{\rm dc}$ (S/cm)	μ_H (cm^2/V s)
73.3	0.084	1000	84
7.3	0.83	136	113
5.2	1.16	110	128
4.5	1.51	99	150
3.3	2.02	80	162
1.8	4.26	57	243
0.89	8.70	40	348
0.34	23.1	25	579

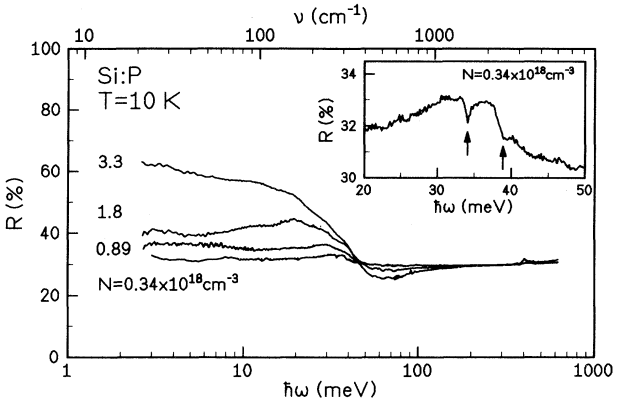

FIG. 2. Reflectance spectra $R(\hbar\omega)$ of the insulating samples at 10 K. The inset gives a magnification of the absorption structures between 20 meV and 50 meV of the sample with the lowest-doping concentration $N = 0.34 \times 10^{18}\,\mathrm{cm}^{-3}$.

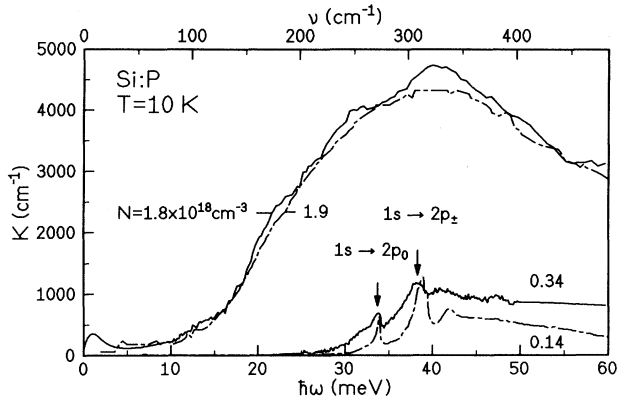

FIG. 4. Absorption coefficient $K(\hbar\omega)$ of two insulating samples obtained from reflection measurements in this paper (solid lines) and, for comparison, from earlier absorption measurements (dashed lines) (Ref. 18).

pletely or partially localized. In contrast to Fig. 1, the spectra now are dominated by broad resonant absorption features having their origin in transitions from the (localized) impurity states to the conduction band. Of particular interest are small dips in the reflectivity between 30 meV and 40 meV, shown in an expanded scale in the inset of Fig. 2 for the lowest-doping concentration. As will be seen later, they are due to transitions into excited impurity states.

The spectra of the metallic samples at the same temperature are displayed in Fig. 3. Again, some weak oscillations, due to experimental artifacts, are visible towards low energies. (In Ref. 4, averaged spectra were shown.) In contrast to the data of the insulating regime, the plasma edges persist, indicating free-carrier absorption at low temperatures. Compared to the spectra at room temperature, the plasma edges become steeper and the shapes of the curves are also changed due to additional interband transitions occurring at 10 K.

Figure 4 shows the absorption coefficients $K(\hbar\omega)$ of two insulating samples (solid lines), which were obtained by performing a Kramers-Kronig transformation of the reflectance spectra at 10 K (Fig. 2) after extrapolation to lower and higher energies, using a Lorentz-Drude model. For comparison, $K(\hbar\omega)$ of two samples with similar doping concentrations (dashed lines) obtained from absorption measurements by Thomas *et al.*[18] is also displayed.

Since there are almost no free carriers at 10 K in the low-doping regime, the refractive index $n(\hbar\omega)$ is constant. In this special case, the absorption processes can be inferred directly from the spectral dependence of $K(\hbar\omega)$. The absorption coefficient of the sample with $N = 0.34 \times 10^{18}\,\mathrm{cm}^{-3}$, the lowest-doping concentration investigated by reflection measurements, shows a broad absorption structure with two sharp peaks at 34 meV and 39 meV corresponding to the dips in the reflectivity in the inset of Fig. 2. These sharp peaks can be attributed to optical transitions $1s(A_1) \rightarrow 2p_0$ and $1s(A_1) \rightarrow 2p_\pm$, respectively.[18] This confirms that at this doping concentration, the donor states can be still described by hydrogenlike wave functions with valley-orbit split $1s$ states and excited states classified by the corresponding angular momentum quantum numbers. The inset in Fig. 5 gives an energetic scheme of some of the impurity levels in the dilute limit. The sharp atomiclike lines correspond to excitations from the ground state to various bound states, where the selection rule $\Delta l = \pm 1$ must be fulfilled. They are followed by a broad absorption band, due to excitations to the continuum (conduction-band) states.[19]

Thomas *et al.*[18] have found a continuous increase of the interaction between donors with increasing doping concentration, resulting in a broadening of the absorption lines accompanied by an asymmetric line-shape. However, our results show that the selection rules mentioned are still valid for $N = 0.34 \times 10^{18}\,\mathrm{cm}^{-3}$. The broad absorption range extending to higher energy may be due to transitions between the ground states and the conduction-band states, broadened due to disorder and electronic correlations.[18]

Although deep in the insulating side, reflection measurements yield very good results as shown by the comparison of the two lower curves of Fig. 4. The absorp-

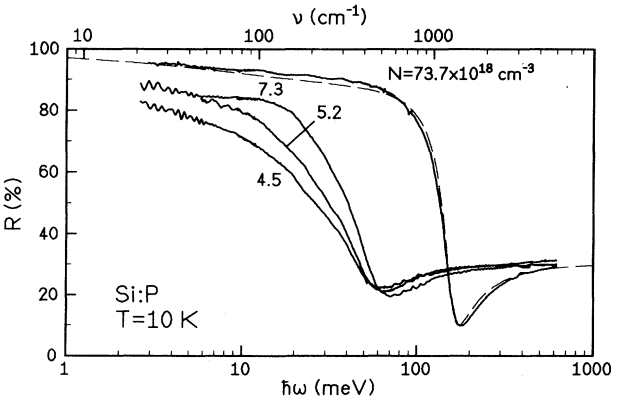

FIG. 3. Reflectance spectra $R(\hbar\omega)$ of the metallic samples at 10 K (solid lines) and Drude fit for $73.7 \times 10^{18}\mathrm{cm}^{-3}$ (dashed line).

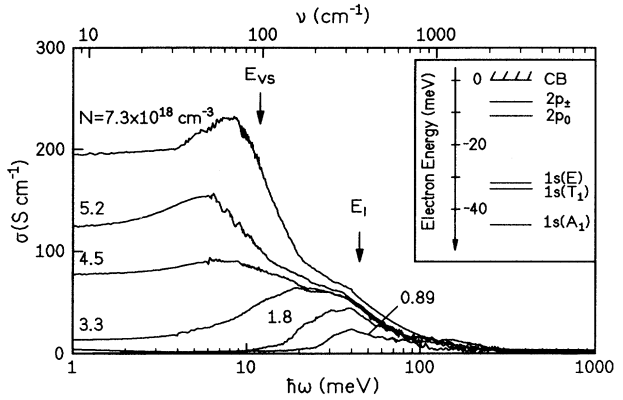

FIG. 5. Conductivity function $\sigma(\hbar\omega)$ of different samples obtained by Kramers-Kronig transformation. The inset gives a sketch of the level scheme of Si:P states in the dilute limit, including valley-orbit splitting of $1s$ states; CB = conduction band; E_I = ionization energy of the impurity atom; E_{VS} = valley-orbit splitting between the $1s(A_1)$ and the closely spaced $1s(T_1)$ and $1s(E)$ levels.

tion coefficient and the asymmetric broadening of the sample with $N = 0.34 \times 10^{18}\,\mathrm{cm}^{-3}$ are larger than of that with $N = 0.14 \times 10^{18}\,\mathrm{cm}^{-3}$, because of the larger number of donors. In the absorption measurements,[18] one more peak was found at approximately 42 meV, which was assigned to the transitions $1s(A_1) \rightarrow 3p_\pm$ and $1s(A_1) \rightarrow 4p_0$ (unresolved due to the small energetic distance). In the spectrum obtained by reflection measurements, these transitions can only be seen as a weak shoulder barely above the noise. Contrary to Thomas *et al.*, no absorption features, due to D^+D^- excitations, were found in our spectra. However, the oscillator strengths of these transitions are very low, resulting in very weak absorption structures in the absorption spectra.[18]

The two upper curves in Fig. 4 show the absorption coefficients of two samples with nearly the same doping concentration, one obtained by the present reflection measurements (solid line), the other from earlier absorption measurements[18] (dashed line). Both agree quite well with each other. The periodic deviations of our data are due to interferences by multiple reflections at the inner cryostat window. The small absorption maximum at very low photon energies is due to a weak contribution of quasifree carriers.

Figure 5 shows the conductivity spectra of the samples from $N = 0.89 \times 10^{18}\,\mathrm{cm}^{-3}$, up to $N = 7.3 \times 10^{18}\,\mathrm{cm}^{-3}$ at 10 K, extending across the critical concentration. The insulating samples exhibit broad peaks near the ionization energy $E_I = 45$ meV of the P atom in Si. With increasing doping concentration, the maximum shifts to lower energy and broadens. In a simple picture, these peaks in $\sigma(\hbar\omega)$ labeled with E_I can be explained by optical transitions from the broadened impurity ground states into the conduction band. For the concentrations in Fig. 5, the optical transitions into excited donor states, which were seen for $N \leq 0.34 \times 10^{18}\,\mathrm{cm}^{-3}$, are masked by the featureless broad absorption due to larger clusters.

At a concentration $N = 3.3 \times 10^{18}\ \mathrm{cm}^{-3}$, i.e., just below N_c, weak contribution of free-carrier absorption can be observed as deduced from the presence of a low-energy tail of $\sigma(\hbar\omega)$. This is in qualitative agreement with specific-heat measurements showing a linear contribution in temperature even below N_c.[20,21] Generally, such a contribution is attributed to free carriers. However, since the dc conductivity is zero for $T \rightarrow 0$, the carriers are not delocalized over the entire crystal. Rather, quasifree carriers confined to clusters would be a possible explanation. However, the only qualitative agreement between "free" carrier concentration below N_c from specific heat and reflectivity calls for further investigations.

For the metallic samples, three different features are observed, which can be assigned to three different absorption mechanisms. First, intraband transitions are present as indicated by the occurrence of well-defined plasma edges in the reflectance spectra of Fig. 3. The spectral weight of this free-carrier absorption increases with increasing doping concentration. Extrapolation of $\sigma(\hbar\omega)$ to $\hbar\omega \rightarrow 0$ yields fairly good agreement with the values of the dc conductivity. The numerical results are compiled in Table III. Second, weak absorption shoulders in $\sigma(\hbar\omega)$ around $E_I = 45$ meV clearly demonstrate that transitions into the conduction band persist even in the metallic state. We interpret these excitations as transitions from the impurity band into the conduction band. Thus, in addition to the free-carrier absorption, these interband transitions can be observed in metallic samples, giving evidence that the metal-insulator transition in Si:P occurs in the impurity band and that the electronic transport at low temperatures is confined to this band, which is well separated from the conduction band.

The energetic position of the impurity band can be inferred from the fitting parameter of the Lorentzian oscillators. For the metallic samples, a choice of 40 meV for the excitation energies $\hbar\omega_0$ describes the spectra at 10 K very well. Although the half widths are of the same order of magnitude (indicating absorption at even lower energies), the energetic distance between the impurity band and the conduction band is approximately 40 meV.

The third and most striking feature in the conductivity function is the strong absorption peak around 7 – 8 meV, which is present in *metallic* samples only (see Fig. 5). This energy is close to the valley-orbit splitting $E_{VS} = 10$ meV between the $1s(A_1)$ and the closely spaced $1s(T_2)$ and $1s(E)$ levels for isolated donors in the dilute limit.[19] (See the inset in the same figure.)

At first sight, it appears surprising that a spectroscopic feature of isolated donors becomes clearly visible only in the metallic regime. However, in the isolated-

TABLE III. Comparison of extrapolated value of $\sigma_{\hbar\omega\rightarrow 0}$ obtained by reflection measurements and the measured value of σ_{dc} at 4 K [measured values after (Ref. 17)].

N (10^{18} cm^{-3})	$\sigma_{\hbar\omega\rightarrow 0}$ (S cm^{-1})	σ_{dc} (S cm^{-1})
73.3	1350	1870
7.3	195	253
5.2	154	147
4.5	78	87

donor regime, this transition is dipole-forbidden due to the angular momentum selection rule $\Delta l = \pm 1$. In principle, the transition $1s(A_1) \rightarrow 1s(T_2)$ is symmetry-allowed and has been observed in the dilute limit in Si:S and Si:Se by Janzén *et al.*[22] However, this effect, which is related to a shallow/deep instability of the $1s(A_1)$ state, has never been observed in Si:P in the very dilute limit. The observation of very weak transitions between the $1s(A_1)$ and the closely spaced $1s(T_2)$ and $1s(E)$ states between $1.2 \times 10^{17}\,\mathrm{cm}^{-3}$ and $1.2 \times 10^{18}\,\mathrm{cm}^{-3}$ by Thomas *et al.*[18] is argued to be due to donor-donor interactions and break down of $\Delta l = \pm 1$. Especially, this is true in the metallic regime, when impurity bands consisting of extended states are formed by overlapping impurity states leading to a complete breakdown of the angular momentum selection rule. Thus, the absorption peaks at about 10 meV constitute unambiguous evidence for transitions between the broadened valley-orbit-split levels in the metallic state of Si:P.

Valley-orbit transitions have been observed in Si:P by Jain *et al.* performing electronic Raman scattering experiments below the critical concentration N_c.[3] In these experiments, it was found that the valley-orbit line $1s(A_1) \rightarrow 1s(E)$ broadens rapidly with increasing impurity concentration and disappears *before* the metallic regime is reached. This different behavior compared to infrared transitions can be understood by taking into account that the selection rules for optical transitions differ from those for electronic Raman scattering in the dilute limit. The selection rules for optical absorption are obtained by first order perturbation theory, whereas for electronic Raman scattering, second order terms must be considered. As a result, optical transitions between the split $1s$ levels are dipole forbidden in the dilute limit, whereas in Raman scattering, the transition $1s(A_1) \rightarrow 1s(E)$ is allowed.[3] The disappearance of the $1s(A_1) \rightarrow 1s(E)$ valley orbit line in the Raman spectrum and the appearance of the optical transitions between the split $1s$ levels show that above the critical concentration N_c, the hydrogenlike wave functions are no longer an adequate description of the impurity states.

Again, the energetic distance and bandwidths of the valley-orbit split $1s$ bands can be inferred from the fitting parameters of the Lorentzian oscillators. Taking the excitation energies for the $N = 7.3 \times 10^{18}\,\mathrm{cm}^{-3}$ sample, we find an energetic distance between the $1s(A_1)$ and the (merged) $1s(T_2)$ and $1s(E)$ bands of approximately 8 meV. The half widths of the oscillators are about 5 meV. This leads to a rough estimate of the $1s(T_2)$, $1s(E)$ bandwidth of approximately this value assuming that the $1s(A_1)$ band is rather narrow.

Finally, reflection measurements on a sample deep inside the metallic regime ($N = 73.7 \times 10^{18}\,\mathrm{cm}^{-3}$) were performed at room temperature (Fig. 1) and at 10 K (Fig. 3). In this doping regime, reflection measurements are a powerful probe, because the large carrier density yield to a distinct plasma edge in the mid-infrared region. At both room temperature and low temperature, the nearly perfect agreement with the Drude fit assigns free-carrier absorption to be the only absorption process present. Even at 10 K, no additional interband transitions occur at about 40 meV or around 10 meV. Consequently, the impurity band and the $1s(T_2)$ and $1s(E)$ levels must have merged at this high-doping concentration.

C. Reflectance spectra at intermediate temperatures

Strong support for the distinct separation of the impurity band and the conduction band in the metallic regime is obtained from an analysis of temperature-dependent reflection measurements on metallic samples. Figure 6 shows the reflectance spectra of the sample with $N = 5.2 \times 10^{18}\,\mathrm{cm}^{-3}$ at various temperatures between 10 K and 300 K. For a clearer display of the absorption shoulders around 40 meV, the $\hbar\omega$ axis is chosen in linear scale. The absorption around 40 meV is independent of T between 10 and 150 K, and then slowly decreases. These absorption structures are due to the interband transitions from the impurity band and the higher $1s$ states into the conduction band.

By fitting Lorentzian oscillators to the spectra, the occupation of the states can be determined (examples of the quality of fits are shown in Fig. 7). Table IV shows values for the excitation energy, the oscillator strength and the half width for each temperature. Assuming that band structure and transition matrix elements are temperature independent, the oscillator strength is proportional to the carrier density in the initial states, i.e., the $1s$ states. This is true, because there is no occupation limit for the final states relevant for the present argument, since the density of states in the conduction band is much larger than in the $1s$ states.

It can be seen from Table IV that at 300 K these states are nearly empty ("exhaustion condition"), i.e., all carriers are thermally excited into the conduction band. It should be noted that it is not the almost perfect agreement with the Drude fit, but rather the *absence* of the absorption structure that leads to this result, since the impurity band is metallic, too. With decreasing tem-

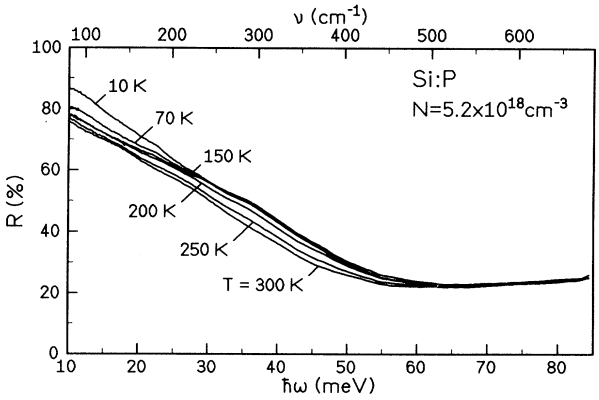

FIG. 6. Reflectance spectra $R(\hbar\omega)$ of the metallic sample with $N = 5.2 \times 10^{18}\,\mathrm{cm}^{-3}$ between 10 K and 300 K. The x axis is chosen in linear scale. Data below 10 meV are not shown, because they exhibit oscillations (cf. Fig. 3).

TABLE IV. Excitation energy $\hbar\omega_0$, oscillator strength $\hbar\omega_p$, half width Γ of the metallic sample with $N = 5.2 \times 10^{18}\,\mathrm{cm}^{-3}$ of the oscillator describing transitions from the $1s$ impurity states to the conduction band as a function of temperature, and deduced occupancy of these states (in %).

T (K)	$\hbar\omega_0$ (meV)	$\hbar\omega_p$ (meV)	Γ (meV)	Occup. of $1s$ states (%)
300	0	0	0	0
250	30	30.0	30	52
200	30	45.0	30	78
150	30	57.5	30	100
10	40	57.5	30	100

perature, the $1s(E)$ and $1s(T_2)$ will be more and more occupied. [The lowest $1s(A_1)$ state is comparatively less occupied, because of the nondegeneracy.] This can be seen from the increase of the oscillator strengths upon lowering the temperature step by step. At 150 K, the conduction band is nearly empty as indicated by the "saturation" of the absorption structure, which does not become stronger at lower temperatures. However, the excitation energy $\hbar\omega_0$ of the Lorentzian oscillators increases from 30 meV at 150 K to 40 meV at 10 K, while the half width remains constant. This can be clearly seen in Fig. 7, where the difference between the reflectance spectra of the sample with $N = 5.2 \times 10^{18}\,\mathrm{cm}^{-3}$ and the Lorentz-Drude fits with $\hbar\omega_0 = 30$ meV and 40 meV are shown at 150 K and 10 K. The deviation of the 30 meV (40 meV) fit from the data for 150 K (10 K) is less than about 1% in the whole frequency range, i.e., much smaller than when interchanging $\hbar\omega_0$. The rise of the excitation energy upon lowering the temperature can be attributed to the increasing population of the lowest $1s(A_1)$ level leading to a larger distance between initial and final states. We

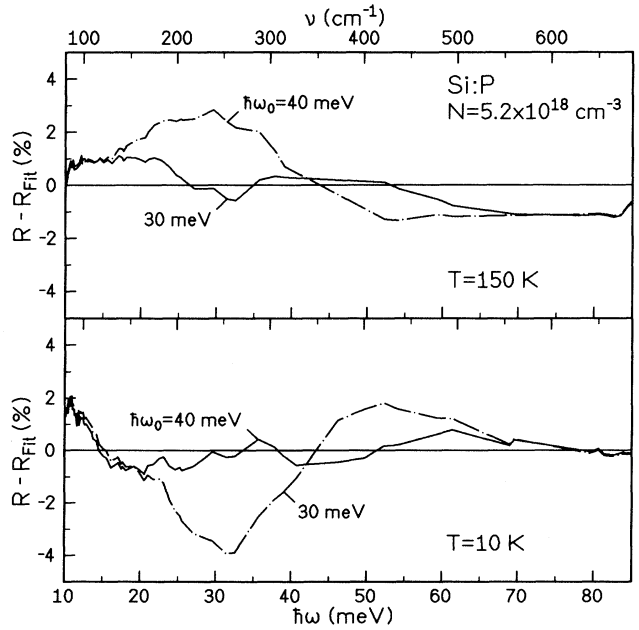

FIG. 7. Difference between the reflectance spectra $R(\hbar\omega)$ of the sample with $N = 5.2 \times 10^{18}\,\mathrm{cm}^{-3}$ and the Lorentz-Drude fits with $\hbar\omega_0 = 30$ meV and 40 meV at 150 K and 10 K.

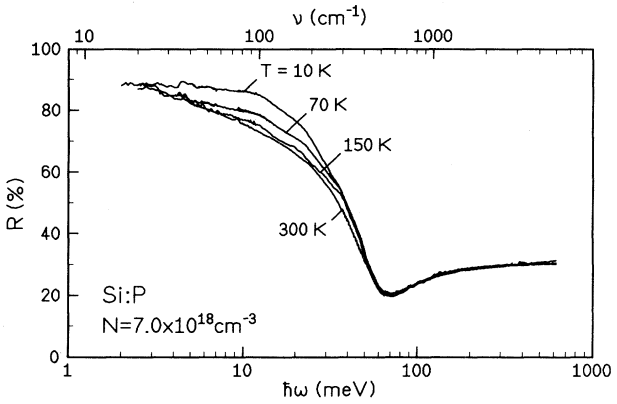

FIG. 8. Reflectance spectra $R(\hbar\omega)$ of the metallic sample with $N = 7.0 \times 10^{18}\,\mathrm{cm}^{-3}$ between 10 K and 300 K.

add that investigation of another metallic sample with $N = 3.8 \times 10^{18}\,\mathrm{cm}^{-3}$ yielded exactly the same features as described here for the $N = 5.2 \times 10^{18}\,\mathrm{cm}^{-3}$ sample. Thus, the temperature-dependent reflection measurements clearly demonstrate that the excitations at about 40 meV are due to transitions of electrons from the impurity band to the conduction band.

On the contrary, the reflectance around 10 meV *does* increase upon lowering the temperature from 150 K to 10 K. The corresponding absorption process is due to optical transitions between the valley-orbit split $1s$ states as discussed above. Again, the occupation of the respective states and bands can be inferred from the temperature-dependent reflection spectra (Fig. 6). While the reflectance below 25 meV hardly differs at 300 K and 150 K, the increase is getting stronger at 70 K reaching a maximum at 10 K. This can be explained by continuous depopulation of the $1s(T_2)$ and $1s(E)$ levels below 150 K (the conduction band being already empty in this temperature range). At the same time, the occupancy of the $1s(A_1)$ impurity band, i.e., the initial state of the corresponding interband transition increases as discussed above.

Figure 8 shows the spectra of another metallic sample with $N = 7.0 \times 10^{18}\,\mathrm{cm}^{-3}$. For this higher concentration, the oscillator strength of the absorption peak around 10 meV is larger, because of the more complete breakdown of the $\Delta l = \pm 1$ selection rule. The behavior of the absorption shoulder near 40 meV, as a function of temperature, is in agreement with the one discussed above for $N = 5.2 \times 10^{18}\,\mathrm{cm}^{-3}$ (Fig. 6). Thus, the change of the occupation within the $1s$ manifold of states leads to the temperature-dependent rise of the reflectance around 10 meV. Since the energy scale of the transitions between the broadened valley-orbit split $1s$ levels is approximately four times smaller than the energy of the transition into the conduction band, the population of the $1s(A_1)$ impurity band should start only at a correspondingly lower temperature, as indeed observed.

V. CONCLUSION

In conclusion, reflection measurements on Si:P performed between 10 K and 300 K provide valuable infor-

mation about various aspects of the metal-insulator transition occurring at $N_c = 3.5 \times 10^{18}\,\mathrm{cm}^{-3}$. At 300 K, all samples show the pure case of free-carrier absorption, where the carriers are thermally activated into the conduction band. The mobilities deduced from a Drude fit can be explained by scattering at ionized impurities and are in agreement with earlier reported dc conductivity measurements.

The low-temperature measurements clearly demonstrate that the MIT in Si:P occurs in the impurity band, which is formed by overlapping of the phosphorous $1s(A_1)$ states. The clearest evidence of this is that central-cell effects are observed even in the metallic phase, i.e., the $1s(A_1)$ and the closely spaced $1s(E)$ and $1s(T_2)$ states are modulating the density of states. This interpretation is supported by temperature-dependent reflection measurements, where all observed structures can be identified unambiguously. The occupation of the respective states and bands could be deduced from the oscillator strengths of the corresponding transitions.

In extension of the work presented here temperature-dependent reflection measurements were performed on compensated Si:(P,B). Metallic samples showed similar behavior as in the uncompensated case. The absorption structure clearly observable around 40 meV and the temperature behavior similar to the uncompensated samples give clear evidence that in compensated Si:(P,B), too, the impurity band is separated from the conduction band when the MIT occurs.

As a final point, we note that no indications of a Mott-Hubbard gap are seen in the present doping regime, in agreement with theoretical predictions.[23]

ACKNOWLEDGMENTS

We thank Dr. W. Zulehner, Wacker Chemitronic, for providing the samples, M. Lakner, H. Stupp, and S. Wagner for the concentration determination, dc conductivity, and Hall effect measurements, R. v. Baltz, F. R. Kessler and, in particular, H. J. Queisser for helpful discussions. This work was supported partly by the Deutsche Forschungsgemeinschaft through Sonderforschungsbereich 195 and by the Commission of the European Communities under Contract No. CI1-0526-M(CD).

* Present address: Fraunhofer-Institut für Angewandte Festkörperphysik, D-79108 Freiburg, Germany.

[1] For a recent review, see, D. Belitz and T. Kirkpatrick, Rev. Mod. Phys. **66**, 261 (1994).
[2] R. L. Aggarwal, Solid State Commun. **2**, 163 (1964).
[3] K. Jain, S. Lai, and M. V. Klein, Phys. Rev. B **13**, 5448 (1976).
[4] A. Gaymann, H. P. Geserich, and H. v. Löhneysen, Phys. Rev. Lett. **71**, 3681 (1993).
[5] F. Wooten, *Optical Properties of Solids* (Academic Press, New York, 1972).
[6] W. R. Thurber, R. L. Matthis, Y. M. Liu, and J. J. Filliben, J. Electrochem. Soc. **127**, 1807 (1980).
[7] S. S. Li and W. R. Thurber, Solid State Electron. **11**, 639 (1968).
[8] W. G. Spitzer and H. Y. Fan, Phys. Rev. **106**, 882 (1957).
[9] M. Cardona, W. Paul, and H. Brooks, Helv. Phys. Acta **33**, 329 (1960).
[10] F. Didley and F. R. Kessler, Phys. Status Solidi B **169**, 141 (1992).
[11] F. R. Kessler (private communication).
[12] S. Reuss, Diploma thesis, Universität Karlsruhe, 1993.
[13] N. F. Mott, Philos. Mag. **6**, 287 (1961).
[14] E. Ohta and M. Sakata, Jpn. J. Appl. Phys. **17**, 1795 (1978).
[15] E. D. Palik and G. B. Wright, in *Optical Properties of III-V Compounds*, edited by R. Willardson and A. Beer, Semiconductors and Semimetals Vol. 3 (Academic Press, New York, 1967).
[16] F. Mousty, P. Ostoja, and L. Passari, J. Appl. Phys. **45**, 4576 (1974).
[17] H. Stupp (private communication).
[18] G. A. Thomas, M. Capizzi, F. DeRosa, R. N. Bhatt, and T. M. Rice, Phys. Rev. B **23**, 5472 (1981).
[19] P. Fisher and A. K. Ramdas, in *Physics of the Solid State*, edited by S. Balakrishna, M. Krishnamurti, and B. Ramachandra (Academic, London, 1969).
[20] N. Kobayashi, S. Ikehata, S. Kobayashi, and W. Sasaki, Solid State Commun. **24**, 67 (1977).
[21] M. Lakner and H. v. Löhneysen, Phys. Rev. Lett. **63**, 648 (1989).
[22] E. Janzén, R. Stedman, G. Grossmann, and H. G. Grimmeiss, Phys. Rev. B **29**, 1907 (1984).
[23] R. N. Bhatt and T. M. Rice, Phys. Rev. B **23**, 1920 (1981).